

Cite this: *Chem. Commun.*, 2011, **47**, 11149–11151

www.rsc.org/chemcomm

COMMUNICATION

Structural reorganization renders enhanced metalloprotein stability†

Hugo M. Botelho and Cláudio M. Gomes*

Received 6th June 2011, Accepted 24th August 2011

DOI: 10.1039/c1cc13354c

The enhanced stability of a mesophilic metalloprotein was assessed using biophysical spectroscopies. Significant local structural inter-conversions during thermal insult account for a reorganization of the protein scaffold, without disturbing the active metal site. This cushioning mechanism is proposed to be a generic property of metalloproteins contributing to enhanced stability.

Understanding the molecular mechanisms underlying protein stabilization is one of the greatest challenges in the protein folding field. The specific set of stabilization strategies which are featured by each protein introduces a degree of complexity which, in most cases, precludes a complete understanding of the coupling between folding energetics, protein structure and stability—a subject of broad relevance and great utility in many fields, from basic science to biotechnological and industrial uses of proteins with enhanced stability.

The spontaneity of the protein folding process has provided the common ground for the analysis of most folding events, with the notable exception of intrinsically unstructured proteins. From high resolution crystallographic structures, solution NMR experiments and theoretical analysis we learnt some of the structural principles underlying the stabilization of the native conformation.¹ Still, the coupling of the protein sequence, folding energetics and native structure remains not fully understood, contributing to the inability of routinely predicting the protein structure (in a given medium): the protein folding problem. This is most striking regarding intrinsically stable proteins originating from organisms thriving at extreme temperature, pressure or salinity. They frequently present identical folds and comparable catalytic efficiency at the optimal temperature to mesophilic counterparts, implying that the enhanced stability lies in subtle adaptations of the polypeptide to the external conditions. Still, there is no single type of adaptation which accounts for all thermostability examples. Instead, thermostability is the outcome of individual contributions such as cofactor binding, increased rigidity, enhanced hydrophobic core packing, larger hydrogen bond networks, oligomerization and shorter loops.¹ A full understanding of how these contributions couple to achieve a specific

structure—the basis of *ab initio* protein design—is still not achievable in all cases, despite the developments in molecular dynamics or human-assisted *in silico* folding.

In this communication we report a study in which biophysical spectroscopy allowed us to establish the coupled contribution of two stabilization strategies in a thermostable protein: nonlocal topology and cofactor binding. We observed that the conformational changes induced by temperature in *Desulfovibrio gigas* rubredoxin (RdDg) at neutral pH are accommodated by the polypeptide, which acquires a non-native β -turn rich structure. The increase of the non-local nature of protein topology[‡] increases unfolding cooperativity and effectively protects the micro-environment of the functionally relevant redox-active iron–sulfur (FeS) center from degradation. We propose that this mechanism buffers the active site from partial misfolding, increasing the apparent protein stability.

Rubredoxin is a 6 kDa protein containing a single iron atom coordinated by four cysteine sulfurs (Fe(Cys)₄), constituting the redox-active moiety of this protein.² The iron cofactor endows the protein with spectroscopic probes (*e.g.* visible and CD absorption) independent of the ones associated with the polypeptide itself (*e.g.* far UV CD and near infrared absorption). All of these are conformation-sensitive and may be used for independently analyzing the integrity and conformation of both the polypeptide and the Fe(Cys)₄ site.

To determine the relative contributions of the iron cofactor and the polypeptide to overall apparent protein stability, we measured the above mentioned spectroscopic signals of RdDg at 25 °C and up to 95 °C during a temperature ramp (Fig. 1A–C). The native (25 °C) RdDg spectra were similar to the ones reported in the literature.^{3,4} The visible absorption and CD bands of the FeS center (Fig. 1A and B) indicate center integrity whereas the far UV CD spectrum (Fig. 1C) shows that the protein is mostly composed of β -sheets and random structures. At 95 °C, the visible absorption decreases by 30%, indicating a quantitative iron loss (Fig. 1A). The same variation is seen in the CD mode (Fig. 1B). The lack of spectral distortion reveals that iron is lost without the formation of detectable intermediates, an all-or-nothing process. Bound iron is kept within the same chiral environment, as reflected by the visible CD bands (Fig. 1B).^{5,6} In this sense, the CD signal decrease just mirrors the cofactor loss. This also indicates that the iron atom keeps the +3 oxidation state, reported by the negative ellipticity at 500 nm⁷ as the Fe^{III}(Cys)₄ moiety is characterized by a negative ellipticity at 315 nm.^{3,5} Further investigations revealed that iron loss, occurring mainly above

Instituto de Tecnologia Química e Biológica, Universidade Nova de Lisboa, Av. República, EAN 2785-572, Oeiras, Portugal.
E-mail: gomes@itqb.unl.pt; Fax: +351 214 411 277;
Tel: +351 214 469 332

† Electronic supplementary information (ESI) available: Materials and methods; FT-IR spectra of RdDg at 20 °C and 94 °C; FT-IR assignments; thermal stability of secondary structure elements. See DOI: 10.1039/c1cc13354c

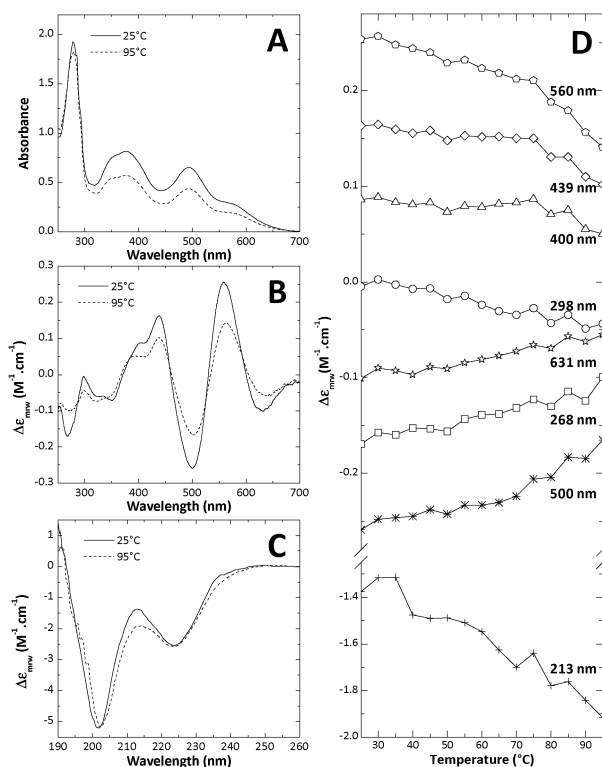


Fig. 1 Monitoring the thermal denaturation of rubredoxin by (A) UV/visible absorption, (B) near UV/visible CD and (C) far UV CD. Spectra were recorded while increasing temperature from 25 (solid lines) to 95 °C (dashed lines). The initial and final spectra are represented. The absorption change at 376 nm suggests a loss of 30% of the iron content. (D) Temperature-induced CD signal variation at specific wavelengths.

70 °C (visible CD, Fig. 1D), was not associated with conformational changes occurring above 50 °C which yielded a β -sheet and β -turn rich conformation at high temperature (see below). Interestingly, the far UV CD spectrum is also kept without major changes at 95 °C (Fig. 1C), denoting no significant change in the overall β -sheet content. This indicates that the rubredoxin fold has a high apparent stability and is able to somehow cushion the effects of the thermal insult. This conclusion is more evident from the fact that the measured thermal transitions are rather monotonic (Fig. 1D). In agreement with previous reports, these changes are irreversible as judged by the invariable spectroscopic signals after re-cooling to 25 °C. This implies that protein stability measurements have a contribution from irreversible unfolding steps and must be referred as apparent stability, rather than thermodynamic stability (the free energy difference between the native and denatured states), which can only be defined for a protein undergoing reversible unfolding.

The accuracy of secondary structure quantification by far UV CD spectroscopy is limited in proteins containing low amounts of helical elements⁸ like rubredoxin, whose structure is mainly composed of random structures (73%) and β -strands (15%).⁹ For such cases, Fourier transform infrared spectroscopy (FT-IR) is the ideal technique due to the quantitative absorption of each secondary structure type at defined positions within the amide I band (1500–1600 cm^{-1}).¹⁰ To achieve a comprehensive conformational description of RdDg during

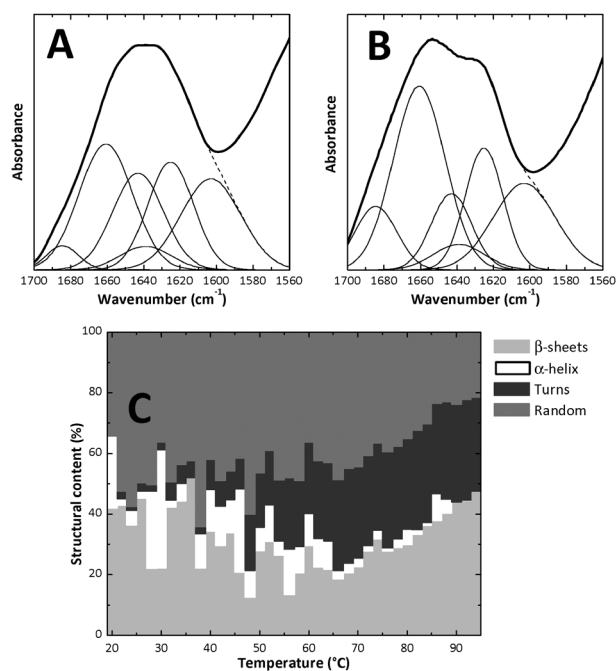


Fig. 2 Analysis of rubredoxin thermal denaturation by FT-IR spectra deconvolution. Spectra recorded at 24 °C (A) and 94 °C (B) are shown as thick solid lines. Spectra were decomposed as the sum of Gaussian bands (thin lines) whose sum (dashed lines) fitted the original spectra. Bands were assigned to secondary structure elements according to reference data.¹⁰ By combining integration with band assignment (Table S1, ESI[†]), a temperature-resolved model of protein secondary structure content was computed (C).

thermal perturbation, we monitored this process using FT-IR. The amide I band maximum of native RdDg is at 1639 cm^{-1} (Fig. 2A), characteristic for β -sheet containing proteins.¹⁰ The spectrum was deconvoluted by placing component bands at second derivative minima (Fig. S1, ESI[†]).¹⁰ Band assignment was based on reference absorption ranges for each type of secondary structure (Table S1, ESI[†]).¹⁰ By monitoring component bands during a 1 °C min^{-1} temperature ramp (Fig. 2) we were able to identify interconversions of secondary structure elements (Fig. 2C) and obtain a detailed temperature-resolved model of the conformational changes occurring along thermal perturbation. RdDg thermal perturbation comprises two regimes: at temperatures up to 60 °C β -sheets unfold, whereas above that point β -sheets (1643 cm^{-1}) and non-native turns (1661 cm^{-1}) build up. There seems to be a transition range (50–65 °C) during which a certain amount of turns are formed ($\sim 30\%$), a value that is kept during the second regime; from that point onwards β -sheet buildup clearly results from random structure reorganization.

The higher protein concentration required for the FT-IR experiment did not affect the overall unfolding behavior, as the visible absorption change was comparable to the one observed before (Fig. 1A) and there was no aggregation. These results thus show that the high apparent thermostability of RdDg resides in the capacity of the polypeptide to accommodate temperature-induced misfolding *via* structural reorganization without affecting the $\text{Fe}(\text{Cys})_4$ moiety. It is worth noticing that the conformational changes observable through FT-IR spectroscopy which were

assigned to holo RdDg likely include a contribution of the unfolded (apo) protein ensemble. However, these measurements are biased towards the folded protein, which accounts for at least 70% of the FT-IR signal at any temperature. In addition, significant amounts of denatured apo protein only occur above 70 °C (visible CD, Fig. 1D), well above the temperature of cushioning onset (~50 °C).

Protein thermostability is the outcome of multiple evolutionary adaptations.¹ In the case of rubredoxin, contributions can be attributed to the polypeptide itself and to the FeS center. The importance of stabilizing the FeS center is highlighted by the extended hydrogen bond networks around this region in the *P. furiosus*¹¹ and *C. pasteurianum* proteins.^{9,11} The three-stranded β -sheet in the rubredoxin fold is crucial in native fold stabilization: all RdDg β -strands include aromatic amino acid residues comprising a major part of the protein hydrophobic core.⁹ The non-local topology of β -sheet proteins increases the cooperativity of the folding (and unfolding) transition and stabilizes the native fold.¹² This means that during temperature increase the native conformation tends to be kept until the vicinity of the midpoint denaturation temperature (T_m). This is not the case with RdDg. The β -sheet component in this protein's structure is small and at neutral pH thermal unfolding is not accessible, even at 95 °C. However, the non-native β -turns assembling during thermal denaturation may provide the conformational resilience responsible for the thermostability of this protein. This is unlike reversible protein denaturation, where activity is lost upon unfolding and recovered under renaturing conditions. Instead, the cushioning mechanism expands the expected temperature range for RdDg activity above the one for *D. gigas* growth (25–40 °C). We cannot rule out that perturbation on small populations could in fact have some degree of reversibility, which remained undetected under experimental conditions. Nevertheless, a cushioning mechanism in proteins with different topologies could indeed have a more prominent reversibility. The localization of the β structures forming at high temperature was not determined. This could be pursued by high temperature NMR,¹³ a technique to which RdDg is amenable.¹⁴

The lack of regular secondary structure elements in native rubredoxins is compensated by the stabilizing incorporation of the iron cofactor, which favors folding.¹⁵ In fact, the loop regions farther from the Fe(Cys)₄ site are the most structurally labile ones in mesophilic and thermophilic rubredoxins.¹⁶ Iron release is the rate limiting step in rubredoxin unfolding¹⁷ and the cause of unfolding irreversibility.¹⁵ Thus, denaturation is determined by polypeptide unfolding. This is corroborated by our analysis: no FeS degradation intermediates are detected, while multiple conformational states are populated. This allows the maintenance of the iron site structure until the polypeptide scaffold stabilization reaches its limit.

The *Clostridium pasteurianum* rubredoxin seems to have similar unfolding properties to those of RdDg. It undergoes major but reversible structural changes below FeS center dissociation temperatures, including lower compactation and local unfolding in the 50–70 °C range, the same one where the *D. gigas* protein exhibits the unfolding regime change.¹⁸ We have shown that these dynamic—and thus destabilizing—regions are reorganized to β -turns at high temperature, validating previous predictions.¹⁹

By accommodating conformational changes at the polypeptide level, the redox-active iron site is kept structurally unaltered, an essential prerequisite for protein function. Since the cluster is solvent exposed in an apical site in native RdDg, conformational changes occurring elsewhere in the protein are not expected to have major effects in recognition of the Fe(Cys)₄ moiety by electron acceptor proteins, also crucial for protein function. Assessing how universal the cushioning strategy is would require a large scale screening of metalloprotein stability, out of the scope of this communication.

Overall, our results illustrate how a polypeptide may evolve in order to accommodate temperature-induced unfolding while preserving the structure of the metal cofactor which is the active site, a mechanism which effectively provides thermostabilization beyond the one arising from the incorporation of the metal cofactor and the intrinsic polypeptide stability alone. The significant residual structure at high temperature may account for some of the protein's thermostability.

This work was supported by grants POCTI/QUI/45758 and PTDC/QUI/70101 (to CMG) from Fundação para a Ciência e a Tecnologia (FCT/MCTES, Portugal). HMB was a recipient of a PhD fellowship (SFRH/BD/31126/2006) from FCT/MCTES. Isabel Pacheco (ITQB/UNL) is gratefully acknowledged for supplying some of the rubredoxin used in this work.

Notes and references

‡ A protein fold has a nonlocal topology when the average sequence separation between contacting residues in the native state is large. This is typical of β -sheet rich proteins.²⁰

- 1 C. Vieille and G. J. Zeikus, *Microbiol. Mol. Biol. Rev.*, 2001, **65**, 1–43.
- 2 C. M. Gomes, G. Silva, S. Oliveira, J. LeGall, M. Y. Liu, A. V. Xavier, C. Rodrigues-Pousada and M. Teixeira, *J. Biol. Chem.*, 1997, **272**, 22502–22508.
- 3 H. E. Christensen, J. M. Hammerstad-Pedersen, A. Holm, G. Iversen, M. H. Jensen and J. Ulstrup, *Eur. J. Biochem.*, 1994, **224**, 97–101.
- 4 D. L. Pountney, C. J. Hennehan and M. Vasak, *Protein Sci.*, 1995, **4**, 1571–1576.
- 5 A. Lombardi, D. Marasco, O. Maglio, L. Di Costanzo, F. Nistri and V. Pavone, *Proc. Natl. Acad. Sci. U. S. A.*, 2000, **97**, 11922–11927.
- 6 A. K. Petros, A. R. Reddi, M. L. Kennedy, A. G. Hyslop and B. R. Gibney, *Inorg. Chem.*, 2006, **45**, 9941–9958.
- 7 W. Lovenberg and B. E. Sobel, *Proc. Natl. Acad. Sci. U. S. A.*, 1965, **54**, 193–199.
- 8 S. M. Kelly, T. J. Jess and N. C. Price, *Biochim. Biophys. Acta, Proteins Proteomics*, 2005, **1751**, 119–139.
- 9 C. J. Chen, Y. H. Lin, Y. C. Huang and M. Y. Liu, *Biochem. Biophys. Res. Commun.*, 2006, **349**, 79–90.
- 10 A. Barth and C. Zscherp, *Q. Rev. Biophys.*, 2002, **35**, 369–430.
- 11 C. M. Bougault, M. K. Eidsness and J. H. Prestegard, *Biochemistry*, 2003, **42**, 4357–4372.
- 12 P. F. Faisca and C. M. Gomes, *Biophys. Chem.*, 2008, **138**, 99–106.
- 13 A. Jung, C. Bamann, W. Kremer, H. R. Kalbitzer and E. Brunner, *Protein Sci.*, 2004, **13**, 342–350.
- 14 P. Lamosa, L. Brennan, H. Vis, D. L. Turner and H. Santos, *Extremophiles*, 2001, **5**, 303–311.
- 15 A. Morleo, F. Bonomi, S. Iametti, V. W. Huang and D. M. Kurtz Jr., *Biochemistry*, 2010, **49**, 6627–6634.
- 16 T. Lazaridis, I. Lee and M. Karplus, *Protein Sci.*, 1997, **6**, 2589–2605.
- 17 S. Cavagnero, Z. H. Zhou, M. W. Adams and S. I. Chan, *Biochemistry*, 1998, **37**, 3377–3385.
- 18 F. Bonomi, D. Fessas, S. Iametti, D. M. Kurtz, Jr. and S. Mazzini, *Protein Sci.*, 2000, **9**, 2413–2426.
- 19 A. Grottesi, M. A. Ceruso, A. Colosimo and A. Di Nola, *Proteins: Struct., Funct., Genet.*, 2002, **46**, 287–294.
- 20 K. W. Plaxco, K. T. Simons and D. Baker, *J. Mol. Biol.*, 1998, **277**, 985–994.

Structural reorganization renders enhanced metalloprotein stability

Hugo M. Botelho^a and Cláudio M. Gomes^{*a}

Electronic Supplementary Information

5 Materials and Methods

Rubredoxin

Desulfovibrio gigas rubredoxin (RdDg) was purified as previously described¹. Protein concentration was determined spectrophotometrically using the visible absorption extinction coefficients $\epsilon^{376\text{nm}} = 8450 \text{ M}^{-1}\cdot\text{cm}^{-1}$ and $\epsilon^{493\text{nm}} = 6970 \text{ M}^{-1}\cdot\text{cm}^{-1}$ ². Purity was verified by the absorption ratio between 377 and 278 nm equaling 0.45. Buffer was 50 mM potassium phosphate at pH 7.

10 UV/visible absorption

UV/visible absorption spectra were recorded using a Shimadzu UV-1700 spectrophotometer at room temperature.

Circular dichroism

CD measurements were recorded in a Jasco J-815 spectropolarimeter equipped with a Peltier-controlled thermostated cell support. 0.1 cm (far UV) and 1 cm (near UV/visible) pathlength cuvettes were used. Thermal denaturation experiments were carried out increasing the temperature from 25 to 95°C at a heating rate of 1°C/min. Every 5°C spectra were acquired. Thermal denaturation was assessed by the CD signal variations at local spectra maxima and minima. Protein concentration was 0.1 mg/ml (17.6 μM , far UV) or 0.62 mg/ml (109 μM , near UV/visible). Far UV CD spectra were accumulated 4 times at 200 nm/min scan rate and 1 s time response. Near UV/visible spectra were accumulated 5 times at 1000 nm/min scan rate and 0.5 s time response.

ATR FT-IR spectroscopy

Attenuated total reflectance Fourier transform infrared spectroscopy (ATR FT-IR) measurements were performed using a Bruker IFS 66/S spectrometer equipped with a nitrogen-cooled MCT detector using the thermostated Harrick BioATR cell II. Protein was concentrated to 10 mg/ml and centrifuged at 12000 g before the temperature ramp to pellet any aggregates forming while concentrating. FT-IR spectra in the amide I (1600-1700 cm^{-1}) and amide II (1500-1600 cm^{-1}) regions were recorded while temperature was increased from 20 to 94°C in a discontinuous fashion: spectra were accumulated during 1 minute (97 accumulations), temperature was raised 2°C during around 45 seconds and sample was equilibrated 15 seconds. Overall temperature change rate was 1.1°C/min. Spectral resolution was 4 cm^{-1} , scanner velocity was 20.0 kHz and aperture was 12 mm. Spectra were analyzed after vector normalization. Spectral variations at specific wavenumbers within the amide I band were assigned to secondary structure changes³. Deconvolution was performed as previously described³. Briefly, the amide I band corresponding to native rubredoxin (20°C) was reconstituted as the sum of gaussian curves centered at second derivative minima. These bands were assigned to secondary structures according to their spectral position³. Then, the component bands' center position was fixed and the remaining spectra were reconstituted by adjusting the curve area and bandwidth. Secondary structure content was estimated from gaussian curve integration.

Structural analysis

The secondary structure content of RdDg was extracted from the crystal structure (2DSX)⁴ using pdbsum (<http://www.ebi.ac.uk/pdbsum/>).

35

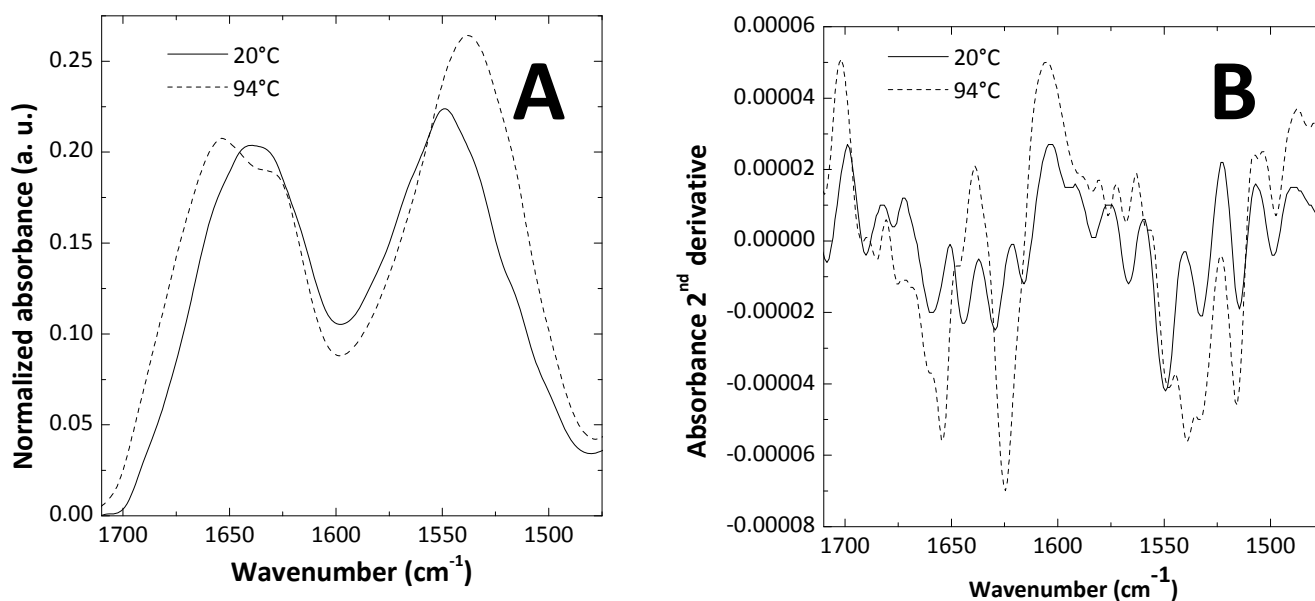
Supplementary tables

Supplementary Table S1. Band assignment for the deconvolution of FT-IR spectra.

| Wavenumber (cm ⁻¹) | Structure |
|--------------------------------|-----------|
| 1684 | β-sheets |
| 1661 | Turns |
| 1643 | Coil |
| 1639 | Coil |
| 1644 | α-helices |
| 1625 | β-sheets |
| 1603 | Mixed* |

*β-sheets and amino acid side chains absorb in this region. Discarded for secondary structure quantification.

Supplementary figures



Supplementary Figure S1. FT-IR monitored thermal denaturation of rubredoxin. Amide I – amide II FT-IR spectra were recorded while increasing the temperature from 20°C to 94°C. (A) FT-IR absorption spectra. (B) Second derivative spectra. The spectra obtained at 20°C (solid line) and 94°C (dashed line) are depicted.

10

Notes and references

^a Instituto de Tecnologia Química e Biológica, Universidade Nova de Lisboa, Av. República, EAN 2785-572, Oeiras, Portugal. Fax: +351 214 411 277; Tel: +351 214 469 332; E-mail: gomes@itqb.unl.pt

1. M. Bruschi, C. Hatchikian, J. Le Gall, J. J. Moura and A. V. Xavier, *Biochim Biophys Acta*, 1976, **449**, 275-284.
2. C. M. Gomes, Universidade Nova de Lisboa, 1999.
3. A. Barth and C. Zscherp, *Q Rev Biophys*, 2002, **35**, 369-430.
4. C. J. Chen, Y. H. Lin, Y. C. Huang and M. Y. Liu, *Biochem Biophys Res Commun*, 2006, **349**, 79-90.

20